ANL/ET/CP-98598

DEVELOPMENT OF MIXED-CONDUCTING CERAMIC MEMBRANE FOR HYDROGEN SEPARATION*

U. Balachandran, T. H. Lee, and S. E. Dorris
Energy Technology Division
Argonne National Laboratory
Argonne, IL 60439

August 1999

Invited paper submitted for presentation at Sixth Annual International Pittsburgh Coal Conference, Pittsburgh, PA, Oct. 11-15, 1999.

*Work supported by the U.S. Department of Energy, Federal Energy Technology Center, under Contract W-31-109-Eng-38.

DEVELOPMENT OF MIXED-CONDUCTING CERAMIC MEMBRANES FOR HYDROGEN SEPARATION

U. Balachandran, T. H. Lee, and S. E. Dorris
Energy Technology Division, Argonne National Laboratory, Argonne, IL 60439

ABSTRACT

The Office of Fossil Energy of the U.S. Department of Energy is formulating "Vision 21," a program aimed at developing technologies for highly efficient power and coproduction plants that discharge almost no pollutants and close the carbon cycle. An integrated gasification combined cycle (IGCC) system is a likely modular component of a Vision 21 coproduction plant. IGCC technology is ideally suited for the coproduction of electricity and high-quality transportation fuel and/or a host of high-value chemicals. As part of the IGCC system, high-temperature membranes for separating hydrogen from coal gasification and other partial-oxidation-product streams are being considered. Thin and dense ceramic membranes fabricated from mixed protonic and electronic conductors provide a simple, efficient means for separating hydrogen from gas streams. Dense mixed-conducting ceramic membranes effect transport via ion- and electron-conducting mechanisms. Because these membranes have no interconnected porosity, selectivity for hydrogen is nearly 100%. Hydrogen separation is achieved in a nongalvanic mode, i.e., without the need for electrodes and external power supply to drive the separation.

$BaCeO_3$-based materials exhibit protonic conductivity that is significantly higher than its electronic conductivity. To enhance the electronic conductivity and increase hydrogen permeation, we have fabricated $BaCeO_3$-containing cermet membranes and used them in a nongalvanic mode to separate hydrogen from gas streams containing H_2, CO, CO_2, and trace amounts of H_2S. Material selection, fabrication, performance as well as technical/technological challenges of the ceramic membranes for hydrogen separation are discussed in this talk.

Keywords

Mixed conductors, hydrogen separation, transport properties, perovskites

INTRODUCTION

The DOE Office of Fossil Energy (FE) sponsors a wide variety of research, development, and demonstration programs to maximize the use of vast domestic fossil resources and ensure a fuel-diverse energy sector while responding to global environmental concerns. Development of cost-effective membrane-based reactor and separation technologies is of considerable interest for applications in advanced coal-based power and fuel technologies. Because concerns over global climate change are driving nations to reduce CO_2 emissions, hydrogen is considered the fuel of choice for both the electric power and transportation industries. Although it is likely that renewable energy sources will ultimately be used to generate hydrogen, fossil-fuel-based technologies will supply hydrogen in the interim.

Outside of direct coal liquefaction, three major industrial areas currently produce and use large volumes of hydrogen; however, other areas, such as hydrogen-fueled vehicles and indirect coal liquefaction, may develop into major users. At present, petroleum refining and the production of ammonia and methanol collectively consume ≈95% of all deliberately manufactured hydrogen in the U.S., with petroleum refining accounting for ≈70%. As crude oil quality deteriorates and restrictions on sulfur, nitrogen, and aromatic levels become increasingly stringent, hydrogen consumption by refineries will continue to increase. All of this will occur while reduced allowances of aromatics in products eliminate hydrogen sources, e.g., naphtha re-forming. In the present climate of growing demand and dwindling sources, membrane technology may reduce refining costs and help retain domestic refining capacity by integrating hydrogen separation and purification into the shift conversion process (thereby facilitating hydrogen production) and by recovering hydrogen from streams where recovery is currently not economical because of low concentration, low pressure, or other factors.

At Argonne National Laboratory (ANL) and the Federal Energy Technology Center (FETC), membranes based on mixed-conducting oxides (i.e., containing both ionic and electronic charge carriers) are being developed for the separation of hydrogen from gas mixtures. Mixed-conducting oxides have been studied for application in many solid-state electrochemical systems such as solid-oxide fuel cells (SOFCs), chemical sensors, and membranes for gas separation [1-7]. One well-known class of mixed conductors contains partially substituted perovskite-type oxides such as $CaZrO_3$, $SrCeO_3$, and $BaCeO_3$, in which substitution of trivalent cations for cerium or zirconium introduces the charged defects that give rise to mixed conduction in atmospheres containing O_2, H_2, and H_2O vapor. These materials exhibit significant proton conduction in a hydrogen-containing atmosphere and are used for various applications, e.g., hydrogen and humidity sensors [3] and solid-oxide fuel cells [4]. In addition, the materials have been used in the dehydrogenation of hydrocarbons, electrolysis of steam, and pumping of hydrogen [5]. To be suitable for hydrogen separation in a nongalvanic mode, i.e. without using electrodes or electrical power, the ceramic membranes must exhibit sufficient protonic and electronic conductivities, and high catalytic activity for oxidation and evolution of hydrogen at the solid/gas interfaces.

The development of dense, hydrogen permeable membranes at ANL/FETC currently focuses on the mixed-conductor yttrium-doped $BaCeO_3$, because its total electrical conductivity (ions and electrons) is among the highest for proton conductors. However, its electronic conductivity is insufficient for nongalvanic hydrogen separation; therefore, cermet membranes are made by mixing this mixed-conductor with various metal powders. The incorporation of a metal phase enhances the electronic conductivity of the membrane and may improve its interfacial catalytic properties. Because of the benefits from the metal, $BaCeO_3$-based cermet membranes provide nongalvanic hydrogen separation. This paper provides an update on the development of $BaCeO_3$-based cermet membranes for hydrogen separation.

EXPERIMENTAL

Preparation of $BaCeO_3$-based ceramic powders and pellets was described in Refs. 8 and 9. Porous electrodes for electrical conductivity measurements were made by applying platinum paste to the surfaces of polished pellets, then firing in air at 1200°C for ≈10 min. Two types of cermet membrane (ANL-1 and ANL-2) were prepared by mixing two metallic powders with $BaCe_{0.8}Y_{0.2}O_{3-\delta}$ (BCY). To prepare cermet membranes that contain 40 vol.% metal, we mixed a metal powder with BCY powder in isopropyl alcohol. The alcohol was evaporated and the resultant powder mixture was pressed into pellets at 200 MPa and sintered at 1400-1420°C for 5 h in 4% H_2/balance argon. After permeation testing, cross sections of the samples were examined with a JEOL JSM 5400 scanning electron microscope (SEM).

Hydrogen permeation through ANL-1 and ANL-2 membranes was measured with the apparatus shown in Fig. 1. Cermet membranes were polished with 600-grit silicon carbide paper and affixed to a support tube by one of several methods. For testing in a feed gas of 4% H_2/balance N_2, ANL-1 membranes of three thicknesses (0.095, 0.144, and 0.205 cm) were attached to an Al_2O_3 tube with a glass sealant. The feed gas in these experiments flowed at a rate of 86 cm^3/min, while the sweep gas (99.995% Ar) flowed over the opposite side of the membrane at a rate of 43 cm^3/min. The effective area of these membranes was 1.4 cm^2. Gas leakage through the setup was tested with 99.995% helium as the feed gas; typical leakage was <10% of the total permeation flux. To obtain more reliable seals for testing in hydrogen, ANL-1 membranes were brazed (Lucas-Milhaupt Handiflo 410) to a short length (5 cm) of Inconel 600 tubing, which was then attached by a stainless steel union to stainless steel tubing for gas manifolding. After determining (by SEM) that the brazing material reacted with the membrane during brazing/permeation-testing and that hydrogen permeation through the metallic support tube itself was significant, this sealing procedure was abandoned.

ANL-2 membranes were then affixed to an Al_2O_3 tube by placing gold rings between the membrane and the tube and heating to 970°C for 5 h, and were tested with 99.995% H_2 and 3.97% H_2/balance helium as feed gases. In these tests, feed gas flowed at ≈100 cm^3/min (3.97% H_2) or ≈200 cm^3/min (99.995% H_2), while sweep gas (103 ppm H_2/balance helium) flowed at 92 cm^3/min. The small concentration of hydrogen in the sweep gas was added to prevent oxidation of the metal in the cermet membrane and was subtracted in calculating the permeation rate. The gas concentrations in the sweep gas were analyzed with a gas chromatograph (Hewlett-Packard 6890) that was periodically calibrated with standard gases.

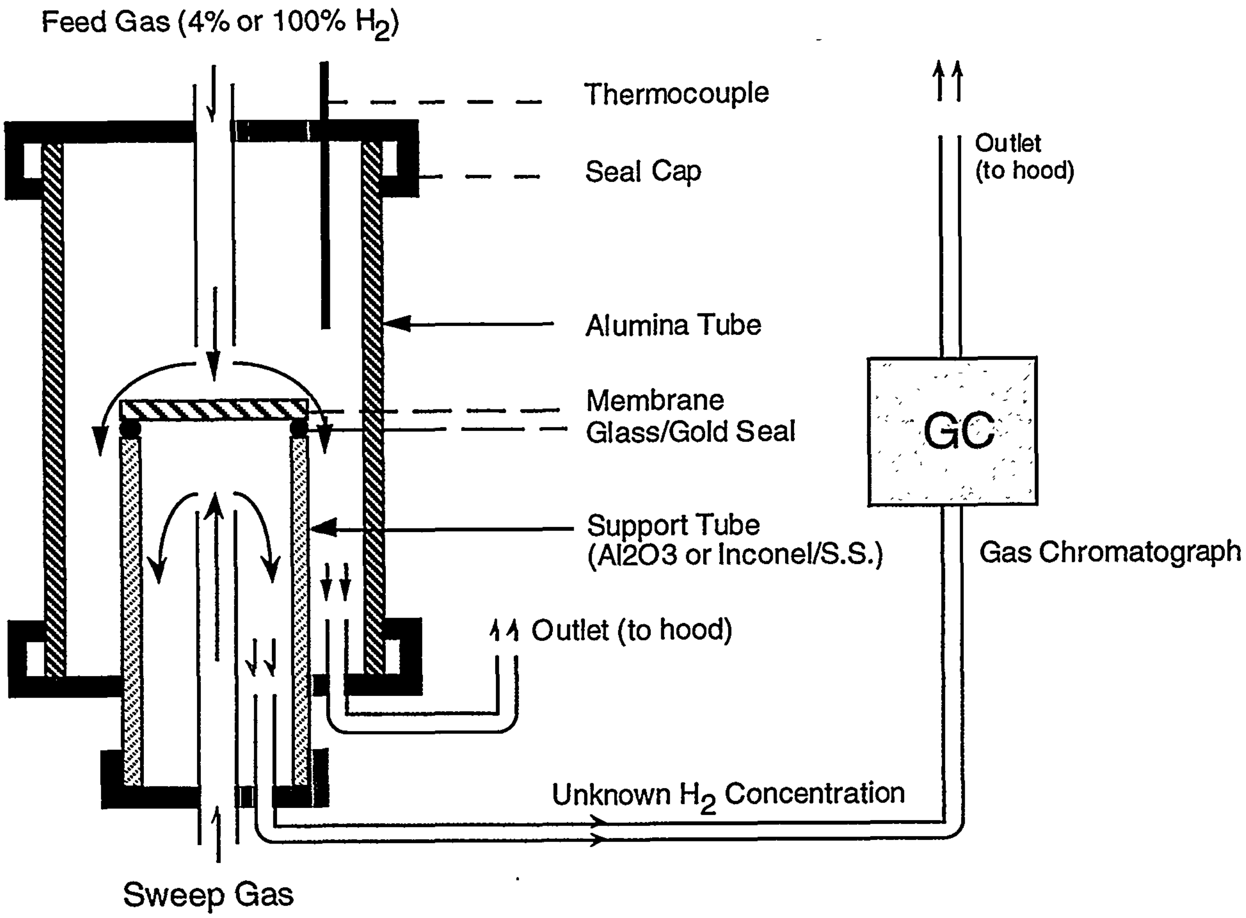

Fig. 1. Schematic illustration of apparatus for measuring hydrogen permeation.

RESULTS AND DISCUSSION

$BaCeO_3$-based materials exhibit total conductivities that are among the highest for proton conductors [10]. Figure 2 shows the total conductivity of $BaCe_{1-x}Y_xO_{3-\delta}$ in 4% H_2/balance N_2 as a function of dopant content x. At a given temperature, conductivity increases with yttrium content over the range $0.0 \leq x \leq 0.20$, then decreases for yttrium content of $0.20 \leq x \leq 0.30$. The increase in conductivity with dopant content may be related to an increase in defect content through the reaction

$$Y_2O_3 \xrightarrow{CeO_2} 2Y_{Ce}' + 3O_O^x + V_O^{\bullet\bullet} ,$$

which would allow BCY to incorporate a higher proton concentration. At higher defect contents, $x > 0.2$, interactions between the defects may reduce defect mobility and decrease the conductivity.

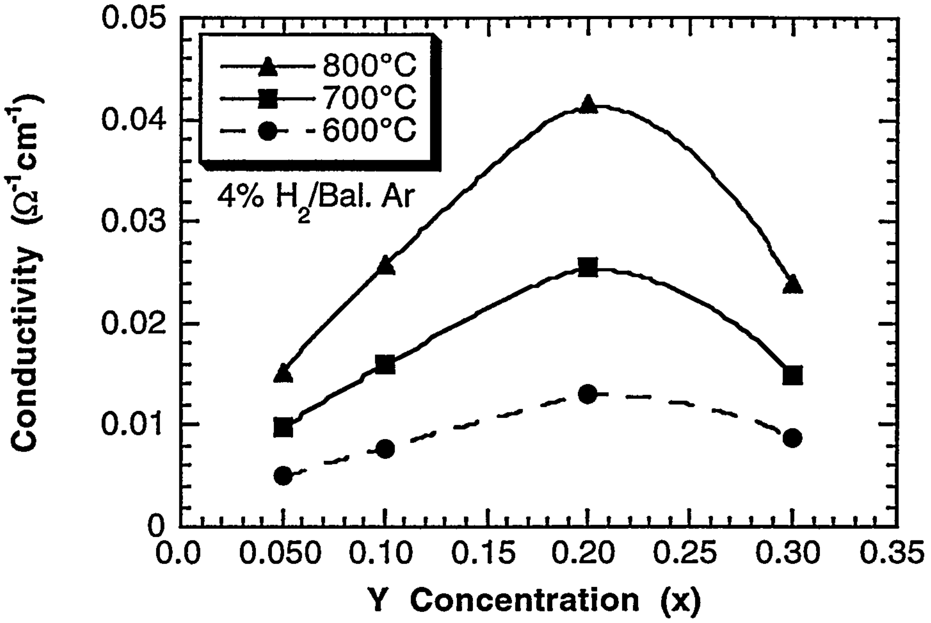

Fig. 2. Conductivity of $BaCe_{1-x}Y_xO_{3-\delta}$ in 4% H_2/balance Ar as a function of yttrium content.

$BaCe_{0.80}Y_{0.20}O_{3-\delta}$ is the most favorable composition for a mixed-conducting membrane because its conductivity is high; however, previous measurements [8] suggest that the fraction of current carried by protons in BCY is significantly larger than that carried by electrons. Because the nongalvanic flux of hydrogen through a mixed-conducting membrane is maximized when the electrons and protons carry nearly equivalent fractions of the current, incorporation of a metal in the BCY should increase the electronic conductivity of the membrane and enhance its performance as a hydrogen separation membrane.

Figure 3 shows the hydrogen permeation rate through ANL-1 cermet (40 vol.% metal) membranes of three thicknesses. The rate of nongalvanic hydrogen permeation N_{H_2} through a mixed-conducting membrane is described [11] by the equation

$$N_{H_2} = \frac{\sigma_{amb}}{2FL}(E_N - \eta), \qquad (1)$$

where L is the thickness of the membrane, F is Faraday's constant, η is the interfacial overpotential, and E_N is the Nernst potential across the membrane. σ_{amb} is the ambipolar conductivity of the membrane, defined as

$$\sigma_{amb} = \frac{(\sigma_{H+}) \bullet (\sigma_e)}{\sigma_{H+} + \sigma_e} \qquad (2)$$

where σ_{H^+} and σ_e are the protonic and electronic conductivities, respectively. The Nernst potential is given by

$$E_N = \frac{RT}{2F} \ln \frac{pH_2''}{pH_2'} , \tag{3}$$

where pH_2'' is the partial pressure of hydrogen in the feed gas and pH_2' is the partial pressure of hydrogen in the sweep gas. Rewriting Eq. 1 as

$$\frac{E_N}{2FN_{H_2}} = \frac{\eta}{2FN_{H_2}} + \frac{L}{\sigma_{amb}} , \tag{4}$$

and plotting the left side of Eq. 4 against sample thickness yields the interfacial polarization resistance, R_p, and the ambipolar conductivity, σ_{amb}:

$$R_p = \left(\frac{E_N}{2FN_{H_2}} \right)_{L \to 0} \tag{5}$$

and

$$\sigma_{amb} = \left[\frac{\partial \left(E_N / 2FN_{H_2} \right)}{\partial L} \right]^{-1} . \tag{6}$$

Fitting R_p and σ_{amb} to Arrhenius-type equations, we calculated the hydrogen permeation rate as a function of temperature and sample thickness.

Hydrogen permeation rates increased with temperature and were approximately proportional to the inverse of membrane thickness (0.095-0.205 cm) at high temperature (800°C), with a slope close to $(E_N\sigma_{amb})/2F$. This result suggests that the bulk properties are rate limiting at high temperatures for samples with thicknesses in the range of 0.095-0.205 cm. The interfacial polarization resistance increases dramatically (activation energy $\approx$1.03 eV) as temperature decreases from 800 to 600°C [12], and the permeation data at low temperatures (<650°C) deviate significantly from the linear dependence on inverse sample thickness. Thus, bulk resistance is much greater than interfacial resistance at high temperature (800°C) for sample thicknesses >0.095 cm, but the interfacial resistance dominates at lower temperatures. This means that reducing the membrane thickness may significantly enhance the permeation rate at higher temperatures but may have little effect at lower temperatures, unless the membrane surfaces are modified to reduce the interfacial resistance.

A metal phase may act to enhance the hydrogen permeation of BCY-based membranes in several ways. It can increase the membrane's ambipolar conductivity by increasing its electronic conductivity and/or it may decrease the interfacial polarization resistance, both of which increase the permeation rate (Eq. 1). Figure 4 shows experimentally measured permeation rates for ANL-2 membranes of three thicknesses. The only difference between ANL-1 and ANL-2 membranes is the composition of the metal phase. The permeation rate through a 1.04-mm-thick ANL-2

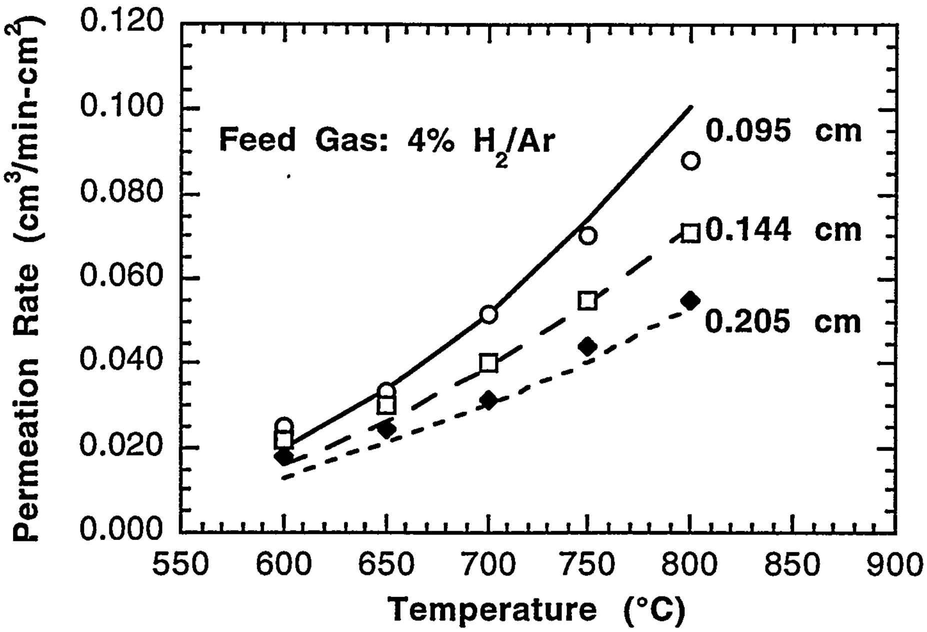

Fig. 3. Rate of hydrogen permeation through ANL-1 cermet membranes of three thicknesses as a function of temperature. Lines represent calculated permeation rates; circles, squares, and diamonds are experimentally measured values.

membrane can be compared directly wtih the calculated permeation rate through an ANL-1 membrane of the same thickness. At low temperatures (T ≤ 700°C), where interfacial polarization dominates, the permeation rate through ANL-2 is significantly greater than that for ANL-1, a finding that suggests that the interfacial polarization resistance of ANL-2 is considerably lower. On the other hand, when bulk properties begin to dominate at high temperatures (T ≥ 800°C), the permeation rate through ANL-1 is greater than that through ANL-2, implying that the ambipolar conductivity of ANL-1 is greater than that of ANL-2 at these temperatures.

The permeation rate through ANL-1 membranes using 99.995% H_2 as the feed gas was measured with two setups. In one setup, the membrane (thickness = 1.6 mm) was brazed to an Inconel support tube. In the other arrangement, where the membrane (thickness = 1.1 mm) was joined to an Al_2O_3 tube by a gold ring, the permeation rate was measured only at 800°C. For comparison, the expected permeation rates through 1.1- and 1.6-mm-thick ANL-1 membranes were calculated with values for R_p and σ_{amb} that were determined earlier. Comparison of the Inconel-measured and -calculated permeation rates through the 1.6-mm-thick sample shows that the measured value is considerably larger than expected, suggesting that significant quantities of hydrogen diffuse through the Inconel/stainless steel fixture. This was confirmed by replacing the

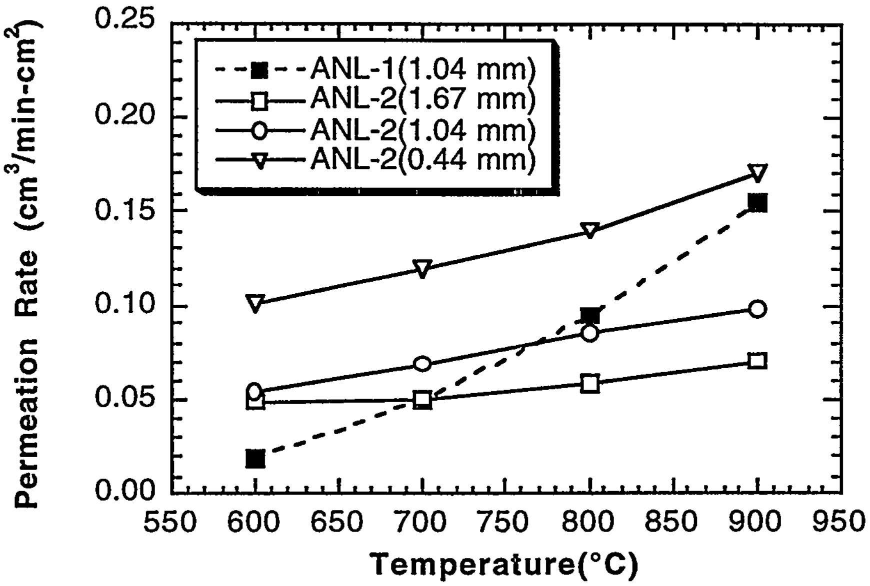

Fig. 4. Permeation rates through ANL-2 membranes of three thicknesses in a feed gas of 4% H_2/balance He. Expected permeation rate for ANL-1 membrane under identical conditions is shown for comparison; lines added as an aid to the eye.

cermet membrane with a stainless steel plug and measuring the permeation rate. Due to its large surface area, the metallic fixture contributes significantly to the apparent permeation rate, even though its permeability is several orders of magnitude lower than that of the BCY-based cermet. By contrast, the agreement between the Al_2O_3-measured and -calculated permeation rates through the 1.1-mm-thick sample is much closer. Because of these data, all subsequent permeation measurements were made with the setup that included the Al_2O_3 tube.

Figure 6 shows permeation data for ANL-2 membranes that were measured with an Al_2O_3 support tube and 99.995% H_2 as the feed gas. The permeation rates through membranes of three thicknesses are given along with the calculated permeation rate for an ANL-1 membrane. The permeation rate through ANL-2 membranes is significantly higher than that for ANL-1 membranes. This is particularly true at lower temperatures ($T \leq 800°C$) and suggests that the metal in ANL-2 significantly reduces the interfacial polarization resistance. This result is consistent with the permeation data that was obtained when 4% H_2/He was used as the feed gas. The highest permeation rate (≈2.1 cm^3/min-cm^2 at 900°C) was obtained with a membrane that was 0.44 mm thick, a thickness that can easily be obtained by extrusion, a conventional ceramic fabrication technique. With another conventional technique that is used to fabricate ceramics, tape casting, even thinner membranes (0.10-0.20 mm) could be made; such membranes should yield permeation rates of 4 to 8 cm^3/min-cm^2 at 900°C.

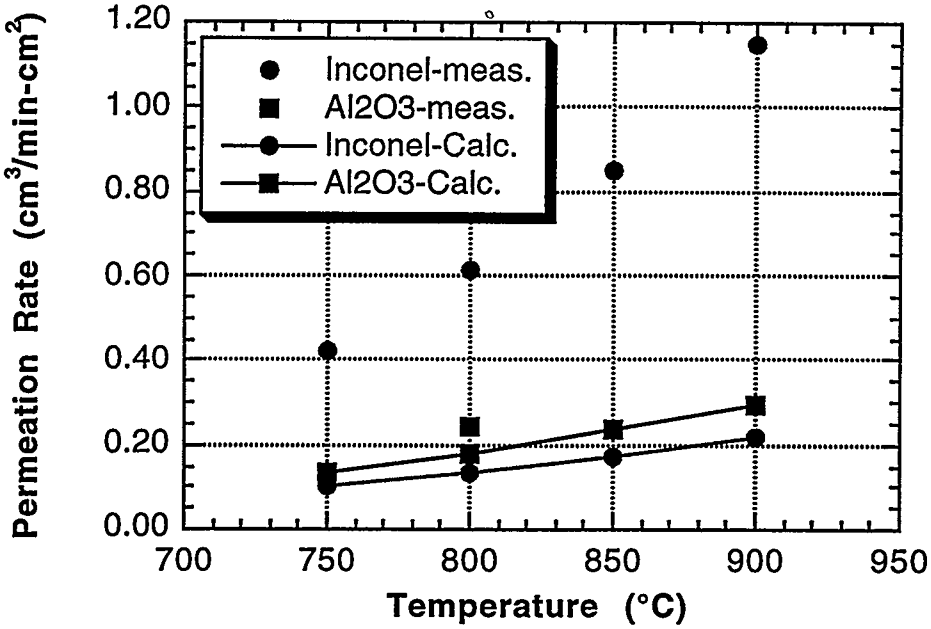

Fig. 5. Permeation rates through ANL-1 membranes, measured with two setups. Feed gas was 99.995% H_2 in both cases. Membrane thickness = 1.6 mm for measurements made with Inconel/stainless steel setup; thickness = 1.1 mm for measurements with Al_2O_3 fixture. For comparison, expected permeation rates are shown by lines.

CONCLUSIONS

$BaCe_{0.8}Y_{0.2}O_{3-\delta}$ (BCY) is a good proton conductor in hydrogen-containing atmospheres, but its electronic conductivity is insufficient to support nongalvanic permeation of hydrogen. Mixing BCY with metal powder reduces its interfacial polarization resistance and increases its ambipolar conductivity, so that BCY-based cermet membranes can be used for nongalvanic hydrogen separation. Two cermet membranes (ANL-1 and ANL-2) with differing metal composition have been made. Although both cermets allow nongalvanic hydrogen permeation, ANL-2 exhibits substantially higher permeation rates than those obtained for ANL-1, particularly at lower temperatures ($T \leq 700°C$). We think that ANL-2 exhibits a higher permeation rate because its metal phase lowers the interfacial polarization resistance; however, additional experiments will be necessary to confirm this.

ACKNOWLEDGMENTS

This work has been supported by the U.S. Department of Energy, Federal Energy Technology Center, under Contract W-31-109-Eng-38. The authors thank Daniel C. Cicero and Gary J. Stiegel, Federal Energy Technology Center, for many useful discussions.

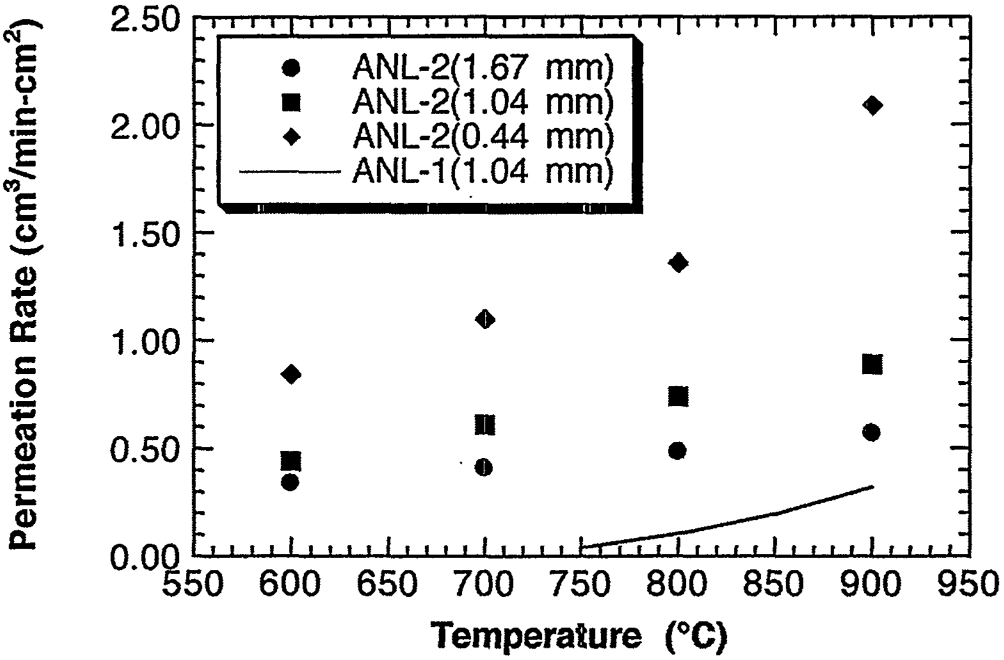

Fig. 6. Measured permeation rates through ANL-2 membranes using 99.995% H_2 as the feed gas for three membrane thicknesses. The line shows the expected, i.e. calculated, value for an ANL-1 membrane under identical conditions.

REFERENCES

[1]. N. Q. Minh and T. Takahashi, "Science and Technology of Ceramic Fuel Cells," Elsevier Science, Amsterdam, 1995.

[2]. H. J. M. Bouwmeester and A. J. Burggraaf, in: Fundamentals of Inorganic Membrane Science and Technology, A. J. Burggraaf and L. Cot, eds., Elsevier Science, Amsterdam, (1996), p. 435.

[3]. N. Fukatsu, N. Kurita, T. Yajima, K. Koide, and T. Ohashi, J. Alloys Comp., **231**, 706-12 (1995).

[4]. N. Taniguchi, E. Yasumoto, T. Gamo, J. Electrochem. Soc., **143**, 1886 (1996).

[5]. J. Langguth, R. Dittmeyer, H. Hofmann, and G. Tomandl, Chemie Ingenieur Technik, **69**, 3197 (1997).

[6]. U. Balachandran, J.T. Dusek, S.M. Sweeney, R.B. Poeppel, R.L. Mieville, P.S. Maiya, M.S. Kleefisch, S. Pei, T.P. Kobylinski, C.A. Udovich, and A.C. Bose, Am. Ceram. Soc. Bull., **74**, 71 (1995).

[7]. H. Iwahara, T. Yajima, and H. Uchida, Solid State Ionics, **70/71**, 267 (1994).

[8]. J. Guan, S. E. Dorris, U. Balachandran, and M. Liu, Solid State Ionics, **100**, 45 (1997).

[9]. J. Guan, S. E. Dorris, U. Balachandran, and M. Liu, J. Electrochem. Soc., **145**, 1780 (1998).

[10]. H. Iwahara, Solid State Ionics, **77**, 289 (1995).

[11]. M. Liu, Proc. 1st Int. Symp. on Ionic and Mixed Conducting Ceramics, T. A. Ramanarayana and H. L. Tuller, eds., The Electrochemical Society, Pennington, NJ, Vol. **91-12**, 215 (1991).

[12]. J. Guan, S. E. Dorris, U. Balachandran, and M. Liu, Presented at Symposium on Electrochemistry of Glass and Ceramics, 100th Annual Meeting and Exposition of the American Ceramic Society, Cincinnati, May 3-6, 1998.